A SYSTEMS ASSESSMENT FOR THE KOREAN ADVANCED NUCLEAR FUEL CYCLE CONCEPT FROM THE PERSPECTIVE OF RADIOLOGICAL IMPACT

JIHAE YOON* and JOONHONG AHN
Department of Nuclear Engineering, University of California, Berkeley
Berkeley, California 94720
*Corresponding author. E-mail : jihae@berkeley.edu

Received December 17, 2009

In this study, we compare the mass release rates of radionuclides (1) from waste forms arising from the KIEP-21 pyroprocessing system with (2) those from the directly-disposed pressurized-water reactor spent fuel, to investigate the potential radiological and environmental impacts. In both cases, most actinides and their daughters have been observed to remain in the vicinity of waste packages as precipitates because of their low solubility. The effects of the waste-form alteration rate on the release of radionuclides from the engineered-barrier boundary have been found to be significant, especially for congruently released radionuclides. The total mass release rate of radionuclides from direct disposal concept is similar to those from the pyroprocessing disposal concept. While the mass release rates for most radionuclides would decrease to negligible levels due to radioactive decay while in the engineered barriers and the surrounding host rock in both cases even without assuming any dilution or dispersal mechanisms during their transport, significant mass release rates for three fission-product radionuclides, ^{129}I, ^{79}Se, and ^{36}Cl, are observed at the 1,000-m location in the host rock. For these three radionuclides, we need to account for dilution/dispersal in the geosphere and the biosphere to confirm finally that the repository would achieve sufficient level of radiological safety. This can be done only after we have known where the repository site would be sited. The footprint of repository for the KIEP-21 system is about one tenth of those for the direct disposal.

KEYWORDS : KIEP-21, KRS, Pyroprocessing, Direct Disposal, Radionuclides Transport

1. INTRODUCTION

In South Korea, currently 20 units, 16 PWRs and four CANDUs, of nuclear power plants are operated. By 2030, 38 nuclear power reactors will be operated with the nuclear share of 59% in electricity generation [1,2]. As nuclear power utilization continues, cumulative mass of Spent Nuclear Fuel (SNF) will also increase. Spent Nuclear Fuel would be considered either as a source of fissile and fissionable materials for re-use as fuel materials or as radioactive wastes for direct disposal [3,4]. In order to continuously utilize the nuclear energy while managing the SNF, the Korea Atomic Energy Research Institute (KAERI) has been developing the pyroprocessing system: Korean, Innovative, Environment Friendly, and Proliferation Resistant System for the 21st Century (KIEP–21) [5-7]. The KIEP-21 system is intended to recover more than 99% of the actinide elements while minimizing the process waste. Toxicity, heat, and volume of the wastes to be loaded in an interim storage and a geologic repository are expected to be significantly reduced by this system. The KIEP-21 would also provide greater flexibility for nuclear material management. A team of researchers in Department of Nuclear Engineering at University of California, Berkeley (UCBNE), recently started a joint research project with KAERI for systems analysis of the KIEP-21 system on proliferation resistance, physical protection, and long-term environmental safety. Among these, this paper reports the results of the environmental and radiological safety analysis.

To make a quantitative evaluation for potential radiological impacts, we need to determine the radionuclide inventory and types of wastes to be generated from the KIEP-21 system as the source terms for the subsequent repository performance analysis. In the present study, for radionuclide inventories in a canister, the number of canisters, and geometries for waste packages, we have utilized the results of the previous studies by KAERI on the mass flow and waste generation from the KIEP-21 system [5-7]. Then, evaluation of the radiological and environmental impacts of the Korean conceptual geologic disposal has been made by the model previously developed at UCBNE [8]. Intermediate-level (ILW) and high-level wastes (HLW) arising from the KIEP-21 system are

significantly different from SNF. We have assumed the Korean Reference repository System (KRS) [9-12] for direct disposal of SNF, while Advanced Korean Reference Disposal System (A-KRS) [13] has been assumed for wastes from the KIEP-21 system. We have evaluated the mass release rates of radionuclides for these two cases at various locations within the engineered barrier region and in surrounding geological media, and observed effects of the waste-form alteration time, T_L, for the pyroprocessing wastes by a parametric study.

The objectives of the present paper are (1) to make a scoping evaluation and comparison for the environmental impacts of geologic disposal, and (2) to survey and identify in which part of the analysis models and data need to be improved toward the ultimate goal of finding an optimized fuel cycle and repository combination. In this paper, we neglect CANDU spent fuel contribution to compare directly between two cases.

2. SUMMARY OF THE STATE

In this section, we summarize the waste streams arising in the KIEP-21 system, based on the previous KAERI studies [5-7]. Then, we make an overview of two repository concepts developed by KAERI, KRS for the direct disposal of SNF, and A-KRS for disposal of five provisional waste streams arising from the KIEP-21 system.

2.1 Five Waste Forms from KIEP-21

From the pyroprocessing of the spent PWR fuel, the provisional five waste streams are generated and solidified into (1) metal waste (ILW), (2) ceramic waste (HLW), (3) vitrified waste (HLW), (4) ceramic waste (ILW), and (5) vitrified waste forms (ILW) [14]. Figure 1 shows the flow sheet and waste streams generated from the KIEP-21 process. In the KIEP-21 system, two different types of salts are used to remove high decay heat fission products and rare earth elements, resulting in LiCl waste salt containing alkali and alkaline-earth fission products (FPs) from the electrolytic reduction process, and LiCl-KCl eutectic waste salt containing rare-earth FPs after TRU drawdown process. Since these waste salts are radioactive, heat-generative, and highly soluble in water, they should be fabricated into durable waste forms that are compatible with the environment in a geologic repository for a final disposal. Stabilization-and-solidification scheme for waste residues from the waste-salt regeneration processes was also developed [15-17]. In this process, high decay heat fission products such Cs, Sr, and rare earth (RE) elements

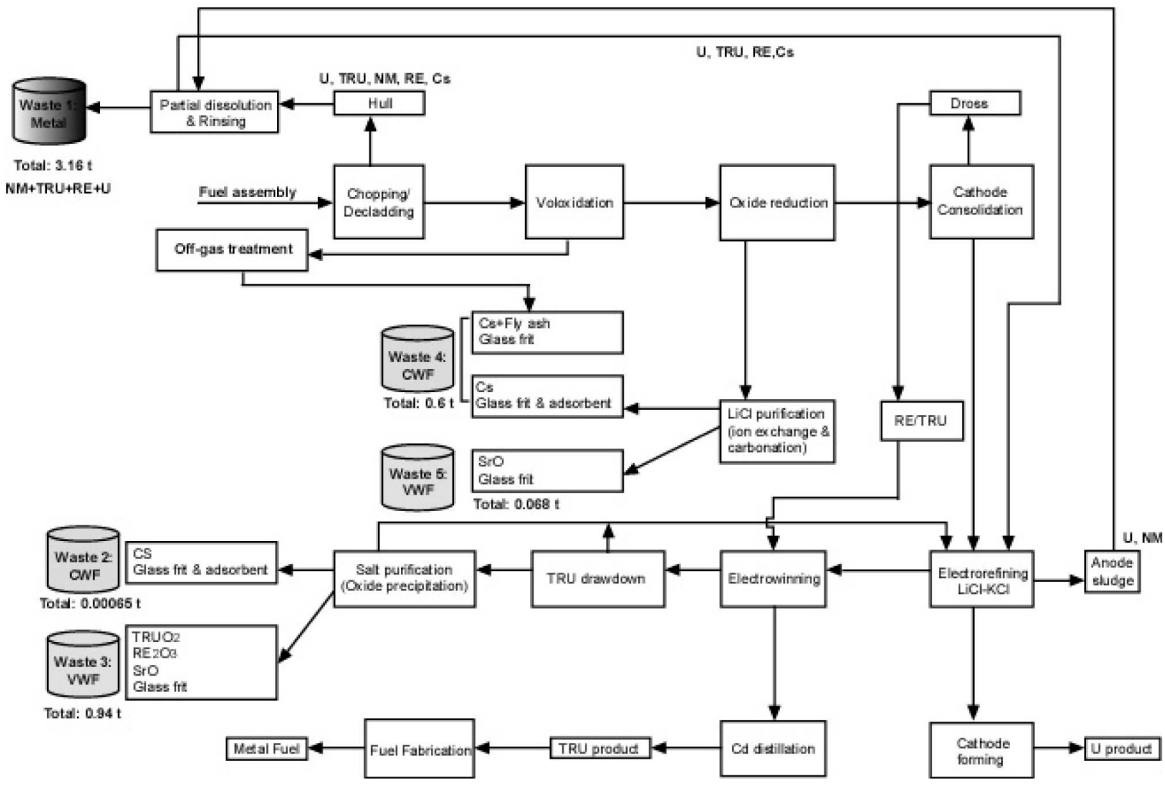

Fig. 1. Flowsheet for Treatment of 10 MTHM of Spent PWR Fuel with 4.5wt% U-235, 45000 MWD/MTU, and 5-year Cooling and Five Provisional Waste Streams

Table 1. Summary for Parameter Values for Waste Forms

	waste stream 1 (Metal)[a]	waste stream 3 (Vitrified)[a]	waste stream 4 (Ceramic)[a]	waste stream 5 (Vitrified)[a]	Spent PWR fuel[b]
Total waste (kg)	3158.53	936.21	600.94	67.99	
Waste Forms Characteristics					
# of blocks for 10 MTU	9.2	1	6	24	
# of blocks/Canister	7 blocks (2.8ton)/can	1 block/can	1 block/can	1 block/can	4 assemblies/ canister
canister dimensions (OD × H)(m)	0.65 × 1.7	0.65 × 1.7	0.216 × 1.31	0.060 × 0.61	1.02 × 4.83
# of blocks for 26,000 MTU	23,920	2,600	15,600	62,400	
# of canisters for 26,000 MTU	3,420	2,600	15,600	62,400	14,788
Package	c-MDP (compact Metal Disposal Package)	SNDC (Storage and Disposal Container)	SR (Storage Racks)	SR (Storage Racks)	
# of Cans/package	4 cans/c-MDP	2 cans/SNDC	6 cans/SR	24/SR	
shape of package	cube	cylinder	hexagonal prism	Cylinder	
package dimensions (m)	1.5 (L) × 1.5 (W) × 1.9 (H)	0.98 (DI) × 3.74 (H)	0.8 (L) × 1.31 (H)	0.45 (DI) × 0.66 (H)	
volume of package (m^3)	4.275	2.821	0.545	0.105	
# of packages	855	1,300	2,600	2,600	
configuration (package) :column ×rows/layers	4 × 80/3	4 × 21/1	4 × 75/1	4 × 165/2	
Repository design					
Disposal depth (m)	200	500 (and 200)	200	200	500
Disposal concept	tunnel/silo	tunnels	tunnels	tunnels	tunnels
# of tunnels	1 tunnel or 1 silo	16 tunnels	9 tunnels	2 tunnels	420 (37 holes/tunnel)
Tunnel dimensions (m)	150 (L) × 8 (W) × 8 (H)				251 (L) × 5 (W) × 6.15 (H)
Porosity of the bentonite region	0.41	0.41	0.41	0.41	0.3
Density of the bentonite region (kg/m^3)	1600	1600	1600	1600	1800
Porosity of the host rock	0.002	0.002	0.002	0.002	0.002
Density of the host rock (kg/m^3)	2650	2650	2650	2650	2700
Porosity of the fractures	0.05	0.05	0.05	0.05	1
Water velocity in the fractures (m/yr)	0.7	0.7	0.7	0.7	0.7
Longitudinal dispersion coefficient	70	70	70	70	70
Tortuosity correction factor for the bentonite*, τ	1	1	1	1	1
Tortuosity correction factor for the host rock*	0.055	0.055	0.055	0.055	0.055
Radius of the equivalent spherical waste, r_1 (m)	0.74	0.59	0.37	0.194	0.60
Radius of the equivalent spherical bentonite region, r_2 (m)	1.34	3.01	1.97	1.2	1.95
Surface area of the waste form, $S = 4\pi r_1^2$ (m^2)	6.88	4.33	1.75	0.47	4.52
Surface area of the bentonite region, $S_2 = 4\pi r_2^2$ (m^2)	22.55	113.79	48.74	18.09	47.76

Fracture aperture, 2b (m)		0.0001	0.0001	0.0001	0.0001	0.0001
Distance between two waste forms		0.76	1.36	1.48	1.72	6.00
Waste-form alteration time, T_L (yr)		4×10^6	4×10^6	4×10^6	4×10^6	4×10^6
Radionuclide Inventory[c]						
Nuclide	Half-Life(yr)[d]	mol/MDP	mol/SNDC	mol/SR	mol/SR	mol/can
^{246}Cm	5.50E + 03	5.32E-04	3.50E-08			3.27E-03
^{242}Pu	3.79E + 05	9.77E-01	6.43E-05			5.93E+00
^{238}U	4.51E + 09	1.18E+03	7.79E-02			7.18E+03
^{238}Pu	8.60E + 01	3.94E-05	2.59E-09			5.35E-04
^{234}U	2.47E + 05	3.37E-01	2.22E-05			2.04E+00
^{230}Th	8.00E + 04	3.38E-05	2.22E-09			2.05E-04
^{226}Ra	1.60E + 03	3.85E-09	2.53E-13			2.44E-08
^{245}Cm	9.30E + 03	3.48E-03	2.29E-07			2.13E-02
^{241}Pu	1.32E + 01	2.55E-26	1.68E-30			2.95E-23
^{241}Am	4.58E + 02	3.46E-01	2.27E-05			2.44E+00
^{237}Np	2.14E + 06	9.41E-01	6.19E-05			5.71E+00
^{233}U	1.62E + 05	1.50E-05	9.85E-10			9.09E-05
^{229}Th	7.34E + 03	1.84E-09	1.21E-13			1.12E-08
^{243}Am	7.95E + 03	2.29E-01	1.51E-05			1.40E+00
^{239}Pu	2.44E + 04	7.51E+00	4.94E-04			4.56E+01
^{235}U	7.10E + 08	1.05E+01	6.90E-04			6.37E+01
^{231}Pa	3.25E + 04	1.71E-06	1.12E-10			1.04E-05
^{227}Ac	2.16E + 01	3.60E-25	2.37E-29			5.41E-23
^{240}Pu	6.58E + 03	3.07E+00	2.02E-04			1.88E+01
^{236}U	2.39E + 07	7.04E+00	4.63E-04			4.27E+01
^{232}Th	1.41E + 10	8.80E-06	5.79E-10			5.33E-05
^{14}C	5.73E + 03		9.66E-02	5.24E-03		2.00E-02
^{36}Cl	3.10E + 05		1.13E-01			2.07E-02
^{59}Ni	8.00E + 04		5.38E-02			4.96E-03
^{63}Ni	9.20E + 01		1.96E-06			3.85E-07
^{79}Se	6.50E + 04		1.65E+00			1.52E-01
^{93}Zr	1.50E + 06	2.06E+00	1.36E+02			1.25E+01
^{94}Nb	2.00E + 04		1.32E-04			1.22E-05
^{99}Tc	2.12E + 05		2.09E+02			1.93E+01
^{107}Pd	7.00E + 06		5.82E+01			5.37E+00
^{126}Sn	1.00E + 05		4.13E+00			3.81E-01
^{151}Sm	8.70E + 01		3.07E-04			6.28E-05
^{135}Cs	3.00E + 06					7.19E+00
^{137}Cs	3.00E + 01					8.27E-10
^{129}I	1.70E + 07					3.49E+00
^{90}Sr	2.81E + 01				3.55E-13	1.07E-10

[a] is based on Refs. [13,31,32]. [b] is based on Refs. [10,30,31].
[c] Inventories included in ILW or HLW generated from a each waste package for pyroprocessing and from a canister for direct disposal at the time of can failure. [d] Half-life data for each radionuclide from Ref. [41]. [*] from Ref. [8].

from the waste salts are generated. These elements are removed in consecutive order from the KIEP-21 process unit [18]. Most of the gaseous fission products (^{3}H, Kr, Xe, I, etc.), volatile metal and metalloid elements (Cs, Rb, Ru, Rh, Mo, Tc, Te, etc.) are sent to the off-gas treatment system at the chopping-decladding and voloxidation processes [7,19]. Then, Sr is recovered in the form of carbonate precipitates from the LiCl waste salt by using Li_2CO_3 during an electroreduction process. Finally, both RE elements and small amounts of actinides in the spent LiCl-KCl waste salt generated after TRU drawdown process are removed in the form of oxide or oxide chlorides by using an oxygen sparging method [18]. The five waste forms are summarized in this section and also in Table 1.

2.1.1 Metal Waste (Waste Stream 1)-ILW

Metal wastes contain effluents from two different processes: (1) cladding hulls from the chopping-and-decladding process and (2) insoluble noble metal fission products from the electro-refiner [19,20]. The first effluent, cladding hulls, are rinsed to remove the adhered fuel and FP materials before being melted to a corrosion-resistant metal alloy. The fissile materials and FPs, except for noble metals, remaining in a hull are dissolved in a LiCl-KCl salt by using zirconium chloride. The second effluent, i.e., the noble metal fission products, contains a small amount of actinides left behind in the anode basket after the electro-refining process. They are also rinsed to remove the actinide elements in the form of chlorides. The rinsed actinide and fission product chlorides are returned to the electro-refiner, while the residual metallic fission products are melted together with the cladding hull and an additional stainless steel to produce a corrosion-resistant metal alloy.

3.16 tons of metal wastes from 10 MTU of spent PWR

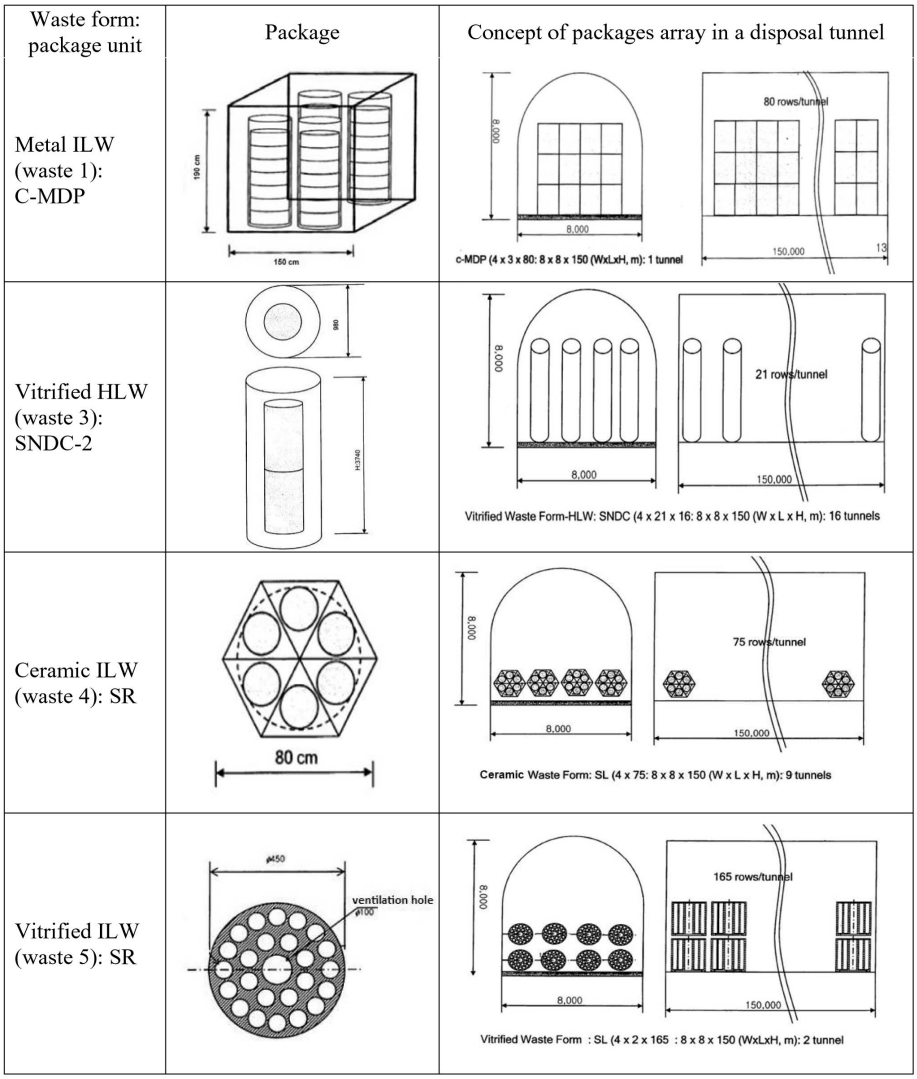

Fig. 2. Schematic Picture of Package and Concept of Packages Array in a Disposal Tunnel [13]

fuel are estimated and conditioned in 9.2 blocks of ingots. 23,920 blocks are expected from 26,000 MTU of spent PWR fuel. In a canister, 7 blocks are placed, and a C-MDP (Compact Metal Disposal Package) contains four canisters for disposal (Fig. 2). Thus, a total of 855 C-MDP are expected for 26,000 MTU of spent PWR fuel.

2.1.2 Ceramic Waste (Waste Stream 2)-HLW

The LiCl-KCl waste salt from the electrowinning process contains a very small amount of ^{135}Cs and ^{137}Cs. 0.00065 tons of ceramic wastes containing mainly Cs isotopes are estimated from 10 MTU. This waste stream will be regarded as HLW because Cs is partitioned from actinides containing the eutectic salt. Detail for the conditioning method is yet to be fixed. Final disposal method will be determined in a future study. In this study, we neglect this waste stream because of the lack of details for the waste generation and solidification, and because of a small amount compared with other streams.

2.1.3 Vitrified Waste (Waste Stream 3)-HLW

The LiCl-KCl waste salt from the electrowinning process contains a considerable amount of rare-earth elements and a small amount of transuranic (TRU) elements and Sr. They are precipitated into their oxide or oxychloride forms via reactions with oxygen gas [21,22]. When the precipitates are fully settled, the upper layer that is mainly composed of LiCl-KCl salt is separated from the precipitate part containing the rare earth elements. The remaining salt in the precipitate phase, which is a mixture of the precipitates and eutectic salt residue, is separated and recovered from the precipitates by using a vacuum distillation/condensation method. Finally, the remaining rare-earth precipitates are converted into stable oxides by a simultaneous dechlorination and oxidation reactions. These are then vitrified with borosilicate glass.

0.94 tons of vitrified waste forms are to be generated from processing of 10 MTU spent PWR fuel, and conditioned in one block. 2,600 blocks are expected from 26,000 MTU of spent PWR fuel. Initial heat generation rate is as high as 4.2 kW/block. 99% of decay heat is generated during the period of 100 years after pyroprocessing. This means that it is efficient to store them for 100 years in an open tunnel. One block of this waste form is encapsulated in a canister, and two canisters are packaged in a SNDC (Storage and Disposal Container) for disposal (Fig. 2). Copper coated SNDC has been proposed. Thus, total 1,300 SNDCs are expected for 26,000 MTU of spent PWR fuel.

2.1.4 Ceramic Waste (Waste Stream 4)-ILW

The LiCl waste salt from the electrolytic reduction process contains Sr and Cs. After recovering and separating strontium by using Li_2CO_3 in LiCl waste salt, small amount of residual Cs is removed from the LiCl waste salt by applying an ion-exchange process with an inorganic material such as zeolite. In addition, 98% of Cs released from the voloxidation process is captured by a fly-ash medium at 650 ºC. Both ^{135}Cs and ^{137}Cs from the voloxidation process and the waste LiCl salt are fabricated to a ceramic waste form with an addition of a solidification agent such as glass frit. This waste form also contains ^{129}I and ^{14}C as well as ^{135}Cs and ^{137}Cs.

0.60 tons of ceramic waste form containing Cs isotopes, ^{14}C, and ^{129}I is generated from 10 MTU and conditioned in six blocks. A block is encapsulated in a canister. Thus, 15,600 blocks of ceramic waste are generated from 26,000 MTU of spent PWR fuel, which are then packaged into 2,600 SRs (Storage Racks). One SR contains 6 canisters (Fig. 2). The initial heat generation rate is 2.0kW/block.

2.1.5 Vitrified Waste (Waste Stream 5)-ILW

Strontium included in the waste LiCl salt from the electrolytic reduction process is solidified by vitrification. First, Sr is precipitated into the form of a carbonate ($SrCO_3$) by addition of Li_2CO_3. Then, $SrCO_3$ separated from the molten LiCl salt is converted into its oxide form (SrO) through a thermal decomposition. Finally, SrO is fabricated to a vitrified waste form.

0.068 tons from 10 MTU of vitrified waste form containing ^{90}Sr is assumed to be conditioned in 24 blocks. Each block is encapsulated in a canister. Thus, 62,400 blocks of vitrified waste are generated from 26,000 MTU of PWR spent fuel, which are packaged into 2,600 SRs (Storage Racks). One SR contains 24 canisters (Fig. 2). Initial heat generation rate is 2.0 kW/block. The diameter of a block is determined by limiting the maximum temperature at the center of the block.

2.2 Repository Concepts

In the present analysis, we consider the repository concepts for disposal of 26,000 MTU of spent PWR fuels or for disposal of wastes resulting from the processing of the same amount of spent PWR fuels by the KIEP-21.

2.2.1 Reference Case for Direct Disposal of Spent Fuels: KRS

KAERI developed the Korean Reference Spent Fuel Disposal System (KRS) based on the current direct disposal policy of SNF generated from both PWR and CANDU since 1997 [10,23,24]. The KRS is similar to the Swedish KBS-3 repository concept [25]. The KRS repository has the single-tier configuration located at the depth of 500 m from the surface, and the multi-barrier system composed of a host geological formation such as granitic rock as the natural barrier system (NBS) [2,10,11]; a waste canister, a bentonite buffer around the canister, and backfilled disposal tunnels are the engineered barrier system (EBS). The Korean Ca-bentonite referred to as 'Gyeongju bentonite' was considered as a candidate buffer material. The waste canister consists of two layers including the corrosion-

resistant copper layer as the outer layer and the inner carbon steel layer to endure the hydraulic pressure and the buffer swelling pressure [10,26-28]. After the emplacement of a canister, the deposition holes are filled with pre-compacted buffer blocks composed of 100% bentonite. Also, the disposal tunnels are backfilled with a mixture of calcium bentonite and crushed rock with the ratio of 30:70 [10].

The repository layout is to be determined primarily by the decay heat of SNF and mechanical strength of the host rock. It is necessary for the peak temperature of the buffer material to be lower than 100 °C to assure the long-term integrity of the engineered barrier. Four assemblies of PWR spent fuel are contained in a canister. Maximum allowable heat generation from the canister is 1,540 W, for which at least a 40 year cooling time in an interim storage before emplacement in the repository is estimated to be necessary [10]. For 26,000 MTU of spent PWR fuel, there will be 14,788 canisters. The distance between the parallel tunnels is 40 m and the minimum distance between two deposition holes for the PWR canisters is 6 m [10]. For the tunnel with dimensions of 251 m long, 5 m wide, and 6.15 m high, 37 canisters will be placed in one tunnel, and thus total 420 tunnels will be necessary for disposal.

2.2.2 Alternative Repository for Five Waste Forms from Pyroprocessing: A-KRS

To accommodate the wastes from the KIEP-21 fuel cycle, the Advanced Korean Reference Disposal System (A-KRS) is being developed by KAERI. Four design goals of A-KRS are [13]: (1) Co-disposal of HLW from pyroprocessing and all levels of wastes contaminated with long-lived radionuclides, (2) Very long-term storage (management) of HLW, (3) Smaller repository footprint per unit electricity generation, and (4) Improved retrievability of emplaced wastes and reversibility for steps toward final closure.

The A-KRS concept is actually combination of an interim storage and a final repository. The system is constructed at two separate depths: 200 meters and 500 meters. Basically, the HLW is to be finally disposed of at the 500-m level, while the ILW is disposed of at the 200-m level. The 200-m level space would also be used as the interim storage for wastes with high decay heat emission. The wastes containing most of short-lived radionuclides such as ^{137}Cs and ^{90}Sr should be stored and disposed of at the 200-m level. Spent PWR fuels would be temporarily stored in the tunnels at the 200-m level before they are processed by the KIEP-21 system. For enhancing the retrievability, the disposal tunnels remain open for at least 100 years before final closure [13].

KAERI has suggested three layout options based on the aforementioned concept. Tunnels with dimensions (150 m long, 8 m wide, and 8 m high) are considered. 855 C-MDPs of the waste 1 (metal) in 1 tunnel, 2600 SRs of waste 4 (ceramic) in 9 tunnels, and 2,600 SRs of waste 5 (vitrified) in 2 tunnels are finally disposed of at the 200 m level, and HLW 2 (ceramic) and 1,300 SNDCs of HLW 3 (vitrified) in 16 tunnels are disposed of at the 500 m level [13].

3. PHYSICAL PROCESSES AND MODEL

In this study, we evaluate the mass release rates (moles of a radionuclide per year) of radionuclides at various locations in the EBS and in the NBS, and compare those between the case of direct disposal of spent PWR fuels in the KRS concept and the case of disposal of wastes from the KIEP-21 pyroprocessing system for the same initial mass of PWR fuel in the A-KRS concept. With the radionuclide release rate, the annual dose to the public is obtained by combining the biosphere pathway analysis.

In this study, we have used the mathematical model, TTB [8], for radionuclide transport through the water-saturated EBS and NBS integrated with the source term model, where precipitation at the waste-form alteration location and subsequent transport of radionuclides in the engineered barriers are modeled. Multiple-member decay chains are taken into account both for the transport in the EBS and NBS and for the source term analysis. In this section, a brief descriptive summary of the TTB model is provided for the reader's convenience. For more detailed mathematical formulations, refer to the previous paper [8].

In a reducing geochemical environment, most actinides will precipitate at the location where they are released from the waste form by alteration of the waste form because of their extremely low solubilities. The radionuclide concentration in groundwater contacting the precipitate of the species is limited by its solubility as long as the precipitate exists. Radionuclides dissolving into the water phase would move away from the precipitate location mainly by molecular diffusion through the water-filled pores in the EBS. We call this the solubility-limited release of radionuclides. On the other hand, the soluble species such as iodine, selenium, and cesium released from the waste matrix can dissolve into the groundwater at the waste form alteration location entirely and then diffuse through the EBS [8]. We call this the congruent release of radionuclides. In this study, metal, ceramic, and borosilicate glass from the pyroprocessing as well as the PWR spent fuel are considered as the waste forms.

Radionuclides released from the waste forms migrate through the EBS. In TTB, the EBS is abstracted as the region around the waste form filled with a porous, water-saturated buffer material. The buffer material serves as a low permeability barrier, allowing only a diffusive solute transport and functions as a filter for colloids, microorganism, and natural organic substances with high molecular weights [26]. Presence of colloids, microorganisms, and natural organic substances are neglected in the analysis of this study, and radionuclides are transported as solutes. The metal canisters containing waste forms and the packages containing the canisters are also neglected in this analysis

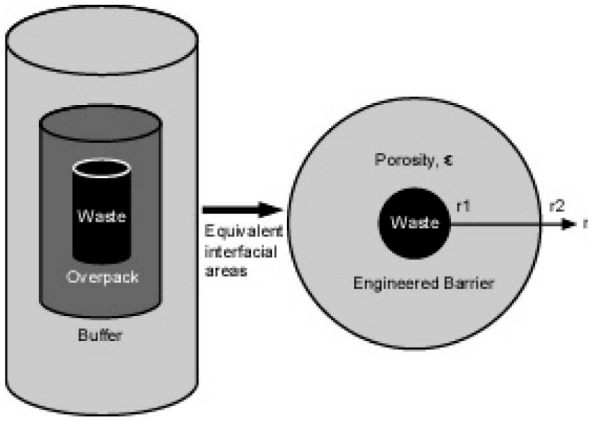

Fig. 3. Conceptual Configuration of the Engineered Barriers

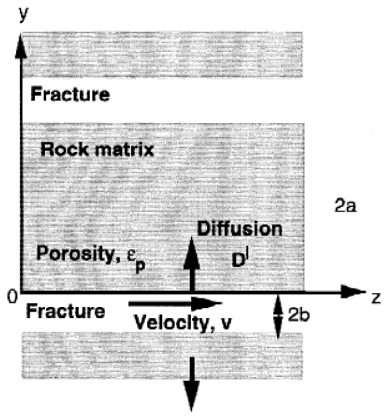

Fig. 4. Conceptual Configuration of Parallel Fractures in the Host Rock. Radionuclides Released from the Engineered Barriers Enter from the Left

[29]. Thus, the waste form is assumed to contact with the porous buffer directly. Radionuclides are assumed to be transported through the porewater in the buffer by molecular diffusion and then through the near-field rock by advection. The hydrological and geochemical conditions within the EBS are assumed constant in time after the beginning of the radionuclide release. In this study, the lifetime of the metal containers for corrosion is conservatively underestimated as 1,000 yr [8]. The radionuclide release by the waste-form alteration is assumed to begin at this point [8].

In the TTB model, the following abstractions and assumptions are made. A waste form has a spherical shape of radius, r_1 (m), surrounded by a uniformly porous region of radius, r_2 (m) (Fig. 3). The waste form alters at a constant rate for the time duration of T_L (yr). Radionuclides in the waste form are released along with the waste form alteration. Radionuclides of low solubility precipitate at r1. Precipitates exist for the time duration of t_k^* (yr). The amount of the precipitate is calculated by the balance of the source terms (the congruent release from the waste form and generation from the precursor by radioactive decay) and the loss terms (the diffusive flux from the precipitate surface and radioactive decay). Multiple isotopes for the same element share the elemental solubility. If the mass balance calculation for the precipitate shows that there exists no precipitate, then that radionuclide is released congruently with the waste-form alteration. This occurs when the nuclide solubility is high, the waste-form alteration is slow, diffusion of the dissolved species in the surrounding porous region is fast, and/or the radioactive decay of the nuclide is fast.

If the aforementioned precipitate mass balance calculation indicates that the precipitate exists, the boundary condition (BC) at the interface r_1 is set as the solubility-limit BC for the time period of t_k^* (yr). After t_k^*, the boundary concentration vanishes. If the precipitate does not exist, the boundary condition at the inner interface r_1 is set as the flux BC by balancing the congruent dissolution rate and the diffusive flux at the interface. For t > T_L, the congruent dissolution rate vanishes. At the r_2 boundary, zero-concentration is assumed for decoupling the transport in the EBS from that in the NBS. With the BCs determined, mass transport in the EBS is calculated based on the governing equation including the diffusion term, radioactive decay term from its mother nuclide, and radioactive decay of itself. Advection in the barrier is neglected.

In the TTB model, for the transport of radionuclides in the NBS, the parallel planar fracture model is adopted [8]. Conceptual configuration of parallel fractures in the host rock is depicted in Fig. 4. The following physical and chemical phenomena in the sub-model for transport in the NBS are considered: (a) advection in the fractures, (b) longitudinal hydrodynamic dispersion in the direction of the fracture axis in the fractures, (c) molecular diffusion in the rock matrix, (d) sorption onto the fracture surface, (e) sorption in the rock matrix, and (f) a radioactive decay chain of arbitrary length [8].

At the interface between the EBS and NBS, the mass conservation is considered for radionuclides. At the outer surface of the spherical EBS (r_2), however, the radionuclide concentration is assumed zero for the transport inside the EBS. This violates the concentration continuity beyond this point in the NBS. Instead, to conserve mass of radionuclides, and to make the assessment conservative, the mass of a radionuclide released at the r_2 surface from the EBS is assumed to be all injected into the planar fractures in the NBS. The number of planar fractures allocated for a single spherical waste form and EBS region is determined by fracture frequency observed in the repository site and the repository tunnel layout.

4. INPUT DATA

Spent PWR fuel initially enriched at 4.5% with a 3 yr

burn up of 45,000 MWd/MTU is assumed to be stored for 5 yrs for cooling before pyroprocessing and 40 yrs for cooling before direct disposal. The ceramic HLW (waste 2) is excluded in this study. The metal waste 1 (ILW) and the vitrified waste 3 (HLW) are assumed to be stored for 100 yrs, and the ceramic waste 4 (ILW) and the vitrified waste 5 (ILW) for 300 yrs before emplacement in the final repository. In either case, we assume 1,000 year before package failure. Thus, wastes 1 and 3 are assumed to start radionuclide release to the EBS region at 1,100 yr, and the wastes 4 and 5 are assumed to start radionuclide release to the EBS region at 1,300 yr after the emplacement. For the direct disposal, spent PWR fuel is assumed to start radionuclide release to the EBS region at 1,000 yr after the emplacement.

Parameter values for the EBS configuration, the barrier properties, and the hydrologic conditions are summarized in Table 1. The values in Table 1 are calculated from the dimension of the conceptual design of Ref. [13] and from the concept of the KRS or obtained by personal communication with KAERI and related literature [10,30-32]. The tortuosity correction factor for the granite host rock and the bentonite are taken from Ref. [8]. The tortuosity correction factor for the bentonite is conservatively assumed to be unity, which overestimates the diffusion coefficients in the bentonite [8,32].

In order to apply the TTB model to KAERI's disposal concepts, we consider waste canisters in a package as a unit for the calculation: e.g., 4 canisters in a C-MDP for waste 1, 2 canisters in a SNDC-2 for waste 3, 6 canisters

Table 2. Assumed Elemental Parameters

Element	Solubility N_e^* (mol/m^3)	In the bentonite				In the host Rock				
		K_d^e (m^3/kg)	D_e (m^2/yr)	K_e (dimensionless)		R_e (1)	K_{dp}^e (m^3/kg)	D_e^I (m^2/yr)	α_e (dimensionless)	
				Pyro-processing	Direct Disposal				Pyro-processing	Direct Disposal
Cu	2.00E-09	3.00E-01	3.20E-02	6.92E+02	1.26E+03	1	4.00E-02	3.52E-06	1.06E+02	1.08E+02
Am	2.00E-09	3.00E-01	3.20E-02	6.92E+02	1.26E+03		4.00E-02	3.52E-06	1.06E+02	1.08E+02
Pu	1.00E-10	3.00E-01	3.20E-02	6.92E+02	1.26E+03		5.00E-01	3.52E-06	1.32E+03	1.35E+03
Np	5.00E-09	1.00E-01	3.20E-02	2.31E+02	4.21E+02		2.00E-01	3.52E-06	5.29E+02	5.39E+02
U	1.00E-08	5.00E-02	3.20E-02	1.16E+02	2.11E+02		1.00E-01	3.52E-06	2.65E+02	2.70E+02
Pa	2.00E-08	5.00E-02	3.20E-02	1.16E+02	2.11E+02		5.00E-02	3.52E-06	1.32E+02	1.35E+02
Th	6.00E-10	3.00E-01	3.20E-02	6.92E+02	1.26E+03		2.00E-01	3.52E-06	5.29E+02	5.39E+02
Ac	3.00E-09	3.00E-01	3.20E-02	6.92E+02	1.26E+03		4.00E-02	3.52E-06	1.06E+02	1.08E+02
Ra	1.00E-06	1.00E-01	3.20E-02	2.31E+02	4.21E+02		2.00E-01	3.52E-06	5.29E+02	5.39E+02
Tc	4.00E-08	1.00E-02	3.20E-02	2.40E+01	4.30E+01		5.00E-02	3.52E-06	1.32E+02	1.35E+02
C	7.00E-05	0.00E+00	3.20E-02	1.00E+00	1.00E+00		1.00E-04	3.52E-06	2.67E-01	2.72E-01
Ni	2.00E-05	5.00E-02	3.20E-02	1.16E+02	2.11E+02		1.00E-01	3.52E-06	2.65E+02	2.70E+02
Pd	3.00E-07	1.00E-03	3.20E-02	3.30E+00	5.20E+00		1.00E-03	3.52E-06	2.65E+00	2.70E+00
Sr	1.00E-04	5.00E-02	3.20E-02	1.16E+02	2.11E+02		5.00E-03	3.52E-06	1.32E+01	1.35E+01
Zr	1.00E-04	2.00E-01	3.20E-02	4.62E+02	8.41E+02		2.00E-01	3.52E-06	5.29E+02	5.39E+02
Cl	-	0.00E+00	3.20E-02	1.00E+00	1.00E+00		0.00E+00	3.52E-06	2.00E-03	2.00E-03
Se	-	0.00E+00	3.20E-02	1.00E+00	1.00E+00		0.00E+00	3.52E-06	2.00E-03	2.00E-03
Nb	-	2.00E-02	3.20E-02	4.71E+01	8.50E+01		2.00E-02	3.52E-06	5.29E+01	5.39E+01
Sn	-	1.00E-03	3.20E-02	3.30E+00	5.20E+00		1.00E-03	3.52E-06	2.65E+00	2.70E+00
Sm	-	2.00E-01	3.20E-02	4.62E+02	8.41E+02		2.00E-02	3.52E-06	5.29E+01	5.39E+01
I	-	0.00E+00	3.20E-02	1.00E+00	1.00E+00		0.00E+00	3.52E-06	2.00E-03	2.00E-03
Cs	-	2.00E-01	3.20E-02	4.62E+02	8.41E+02		5.00E-02	3.52E-06	1.32E+02	1.35E+02

in a SR for waste 4, and 24 canisters in a SR for waste 5. The volume of the EBS region (abstracted as the porous buffer in TTB) associated with the unit is calculated by the dimensions of a disposal tunnel divided by the number of waste packages allocated in a tunnel (Fig. 2). The repository tunnel with tunnel crown space is simply assumed as rectangular prism. The radii of the equivalent-sphere waste package and the porous buffer region are calculated based on the dimensions of the cylindrical waste package and the buffer region, which have the same interfacial areas proposed in Ref. [8] and shown in Fig. 3. We neglected internal structures in each waste package, i.e., C-MDP, SNDC-2, and SR, and only abstracted them as the homogeneous spherical waste form. In case of KRS, the deposition hole area, which is composed of canisters and buffer material beneath the disposal tunnel, are considered as EBS, and disposal tunnel filled with backfill material is not considered. In this study, the excavation disturbed zone (EDZ) is not considered in either concept of the repositories.

The waste-form alteration time T_L is set as 4 million years for the spent PWR fuel in this comparison. For the four waste forms from the pyroprocessing, we assume three cases: 10,000 years, 100,000 years and 4 million years. This simplification is made due to the lack of detailed specification and knowledge for the waste form durability in repository environment, especially for the pyroprocessing waste forms, also partly due to the fact that the repository site is unknown. For the spent PWR fuel, however, the 4 million year alteration time is considered a reasonably conservative estimate. One important characteristic that has not been considered in this study for spent PWR fuel is potential instantaneous release of fission gasses and volatile elements stored in the rim region of the fuel pellet and the gap between the pellet and the cladding. Iodine would be released very early after the canister failure in a pulse-like fashion in this case [33-37]. Table 1 shows the radionuclide inventory in each waste form. We consider four decay chains for actinides. Fission-product radionuclides such as ^{14}C, ^{36}Cl, ^{59}Ni, ^{63}Ni, ^{79}Se, ^{90}Sr, ^{93}Zr, ^{94}Nb, ^{99}Tc, ^{107}Pd, ^{126}Sn, ^{129}I, ^{135}Cs, ^{137}Cs, and ^{151}Sm are also considered.

Table 2 summarizes the parameter values assumed for each element included in waste forms of the pyroprocessing and spent PWR fuel. Solubilities have been obtained in Ref. [32]. The authors are aware that these solubility values were obtained for the case of disposal of vitrified HLW from PUREX reprocessing in a similar water-saturated repository. Because there would be different coupled interactions among chemical species dissolving from differing waste forms, EBS materials, groundwater, and radionuclides, solubility values should be determined for each combination of a waste form and EBS configuration. Sorption distribution coefficient data for the bentonite and for the granitic rock are also taken from Ref. [26,30,32]. The same thing as that for the solubility mentioned above can be said for the values of sorption distribution coefficients. The retardation coefficient for the fracture transport is set to be unity by assuming conservatively that no nuclide is sorbed by the fracture-filling materials.

5. NUMERICAL RESULTS

In this section, we summarize the numerical results for the radionuclide release rates at the surface of the spherical waste form, at the outer boundary of the EBS, and at various locations in the NBS for the waste forms considered above. Comparison has been made to observe effects of different waste forms and effects of waste-form alteration rates. Based on the radionuclide release rate, we also evaluate the annual dose with common biosphere dose conversion factors, and compare the results with the existing Korean regulatory guidelines for radiological safety.

5.1 Mass Release Rates for 4 Million Year Alteration Time

In this section, we observe the results for the cases with 4 million year alteration time, T_L, for all waste forms including spent PWR fuel. Figures 5 through 8 show the results for the pyroprocessing wastes and spent PWR fuel. In each of these figures, Figure (A) shows the congruent release rate of radionuclides, and Figure (B) shows the release rate of each radionuclide at the interface (r_1) between the spherical waste form and the porous buffer region. The difference between (A) and (B) is considered to be precipitated at the interface. If the curves are identical between (A) and (B) for some radionuclides that means those nuclides are released congruently. Figure (C) is the release rate observed at the outer surface of the EBS. Figures (D), (E), and (F) are those observed at 10, 100, and 1000 m locations in the planar fracture intersecting the NBS. In all figures, the horizontal time axis shows the time elapsed after the package failure.

5.1.1 Metal Waste (Waste Stream 1)-ILW

The metal waste form has noble metals, transuranic elements, rare-earth fission product, and uranium. Most actinides and their daughters have the solubility-limited boundary condition except ^{226}Ra, ^{241}Pu, and ^{227}Ac as shown in Table 3. Therefore, most of them released from the waste form are considered to precipitate in the vicinity of the waste form location due to their extremely low solubilities. At the inner boundary ($r = r_1$), ^{93}Zr is the dominant radionuclide (Fig. 5(B)). Most actinides and their daughters disappear already at the outer boundary of EBS. After diffusion in the EBS region, only ^{93}Zr is observed at the EBS surface, $r = r_2$. Figure 5 (D) shows the mass release rate of radionuclides from a single waste package (i.e., MDP) at 10-m location away from the EBS surface as a function of time. ^{93}Zr is observed at the 10-m

Table 3. Determined Boundary Conditions for Different Waste-Form Alteration Time

Nuclide	t_k^* (yr)			t_k^* (yr)			t_k^* (yr)			
	$T_L = 1 \times 10^4$ yr			$T_L = 1 \times 10^5$ yr			$T_L = 4 \times 10^6$ yr			
	waste 1	waste 3	waste 4	waste 1	waste 3	waste 4	waste 1	waste 3	waste 4	SNF
^{246}Cm										
^{242}Pu	9.57E+06	4.48E+06		9.11E+06	4.02E+06		8.57E+06	3.39E+06		9.28E+06
^{238}U	1.00E+10	2.84E+09		1.00E+10	2.85E+09		1.00E+10	2.85E+09		1.00E+10
^{238}Pu	C	C		C	C		4.00E+06	C		4.00E+06
^{234}U	6.52E+06	3.24E+06		6.57E+06	3.29E+06		9.55E+06	6.29E+06		1.00E+07
^{230}Th	1.10E+06	7.71E+04		1.41E+06	3.34E+05		5.19E+06	4.11E+06		5.34E+06
^{226}Ra	C	C		C	C		C	C		C
^{245}Cm	1.24E+05	C		1.23E+05	C		6.89E+04	C		9.31E+04
^{241}Pu	C	C		C	C		C	C		C
^{241}Am	1.44E+04	5.14E+03		7.93E+04	3.53E+03		2.98E+04	C		4.81E+04
^{237}Np	3.08E+07	3.66E+06		3.09E+07	3.70E+06		3.09E+07	3.28E+06		3.51E+07
^{233}U	C	C		3.23E+07	6.18E+06		3.20E+07	5.60E+06		3.63E+07
^{229}Th	3.05E+05	6.91E+04		2.21E+05	1.23E+05		4.10E+06	3.52E+06		4.11E+06
^{243}Am	1.55E+05	4.91E+04		1.54E+05	3.73E+04		1.14E+05	C		1.33E+05
^{239}Pu	6.90E+05	3.63E+05		6.91E+05	3.64E+05		6.54E+05	2.99E+05		7.07E+05
^{235}U	1.00E+10	1.53E+09		1.00E+10	1.54E+09		1.00E+10	1.54E+09		1.00E+10
^{231}Pa	1.23E+05	C		2.79E+05	C		4.03E+06	C		4.10E+06
^{227}Ac	C	C		C	C		C	C		C
^{240}Pu	1.96E+05	1.09E+05		2.05E+05	1.18E+05		1.84E+05	8.91E+04		1.99E+05
^{236}U	4.74E+08	1.60E+08		4.74E+08	1.60E+08		4.76E+08	1.62E+08		5.22E+08
^{232}Th	2.43E+09	1.32E+05		1.00E+10	1.96E+06		1.00E+10	2.88E+07		1.00E+10
^{14}C		3.52E+04	1.36E+04		2.37E+04	C		C	C	C
^{36}Cl		C			C			C		C
^{59}Ni		2.45E+05			2.46E+05			C		C
^{63}Ni		C			C			C		C
^{79}Se		C			C			C		C
^{93}Zr	2.68E+06	1.20E+07		2.68E+06	1.20E+07		1.01E+06	1.20E+07		5.03E+06
^{94}Nb		C			C			C		C
^{99}Tc		4.83E+06			4.83E+06			4.84E+06		3.80E+06
^{107}Pd		9.15E+07			9.15E+07			9.15E+07		5.75E+07
^{126}Sn		C			C			C		C
^{151}Sm		C			C			C		C
^{135}Cs			C			C			C	C
^{137}Cs			C			C			C	C
^{129}I			C			C			C	C

* Letter C means that no precipitate occurs and the congruent release boundary condition is applied
* Shaded areas represent no application of the radionuclide

location, but disappears at locations farther than 10 m. This result shows the EBS and relatively short distance in NBS can effectively confine radionuclides in the metal waste form.

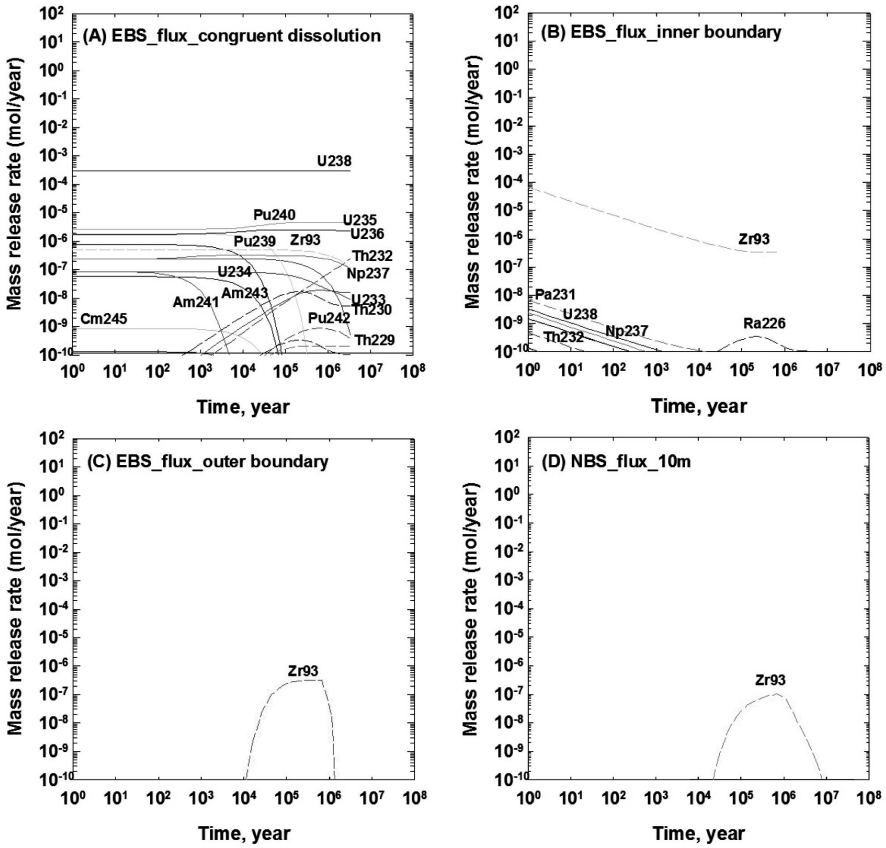

Fig. 5. The Mass Release Rate of Radionuclides for Waste Stream 1 at the Surface of the Metal Waste Form, the EBS Region, and at the Natural Barrier. Transport Distance through the Fractures is 10 m. The Waste-form Alteration Time is Assumed to be 4,000,000 yr. Figure (E) or (F) is not Shown Here because the Value is too Small to Show

5.1.2 Vitrified Waste (Waste Stream 3)-HLW

The high-level vitrified waste (waste stream 3) contains a considerable amount of rare-earth elements as major nuclides and a small amount of TRU and Sr because most uranium and TRU are recovered through pyroprocessing. Actinides, their daughters, and fission products with long half-lives have the solubility-limited boundary condition as shown in Table 3. On the other hand, the congruent release boundary condition is applied to actinides, their daughters, and fission products with relatively short half-lives. Of the fission products considered here, only zirconium, technetium, and palladium have the solubility-limited boundary condition and rest of them are congruently released from the waste matrix (Fig. 6 (A) (B)). Most of fission products disappear at the outer boundary of EBS, while ^{79}Se, ^{126}Sn, ^{36}Cl, ^{14}C, ^{107}Pd, and ^{93}Zr, which have long half-lives, high solubility, and no or very weak sorption survive diffusion in the EBS region with about two orders of magnitude reduction on the mass release rate at the outer boundary of EBS compared to that of the inner boundary of EBS. Figure 6 (D) through (F) show the mass release rate of radionuclides from a single waste package (i.e., SNDC-2) at locations at 10 m, 100 m, and 1000 m away from the EBS surface as a function of time. The major contributions are ^{126}Sn, ^{79}Se, ^{36}Cl, ^{93}Zr, ^{14}C, and ^{107}Pd at 10-m location and ^{126}Sn, ^{79}Se, and ^{36}Cl at 100-m location. At the 1000-m location, two orders of magnitude reduction is achieved for the residual radionuclides such as ^{79}Se and ^{36}Cl.

5.1.3 Ceramic Waste (Waste Stream 4)-ILW

The intermediate-level ceramic waste form (waste 4) contains ^{129}I and ^{14}C as well as ^{135}Cs and ^{137}Cs. As shown in Table 3, they are released from the waste form congruently with the waste-form alteration. Because the half-lives of ^{137}Cs and ^{14}C are relatively short compared with the waste-form alteration time, the majority of ^{137}Cs and ^{14}C decay out while in the waste form. Because of high solubility and the long half-lives of ^{129}I and ^{135}Cs, they are released from the waste form. Especially, ^{129}I is the major contributor at the EBS surface, $r = r_2$, because of its long half-life, high solubility, and no sorption with the bentonite (Fig. 7(C)). Figure 7 (D) through (F) show the mass release rate of radionuclides from a single waste package (i.e., SR) at locations at 10 m, 100 m, and 1000 m away from the EBS

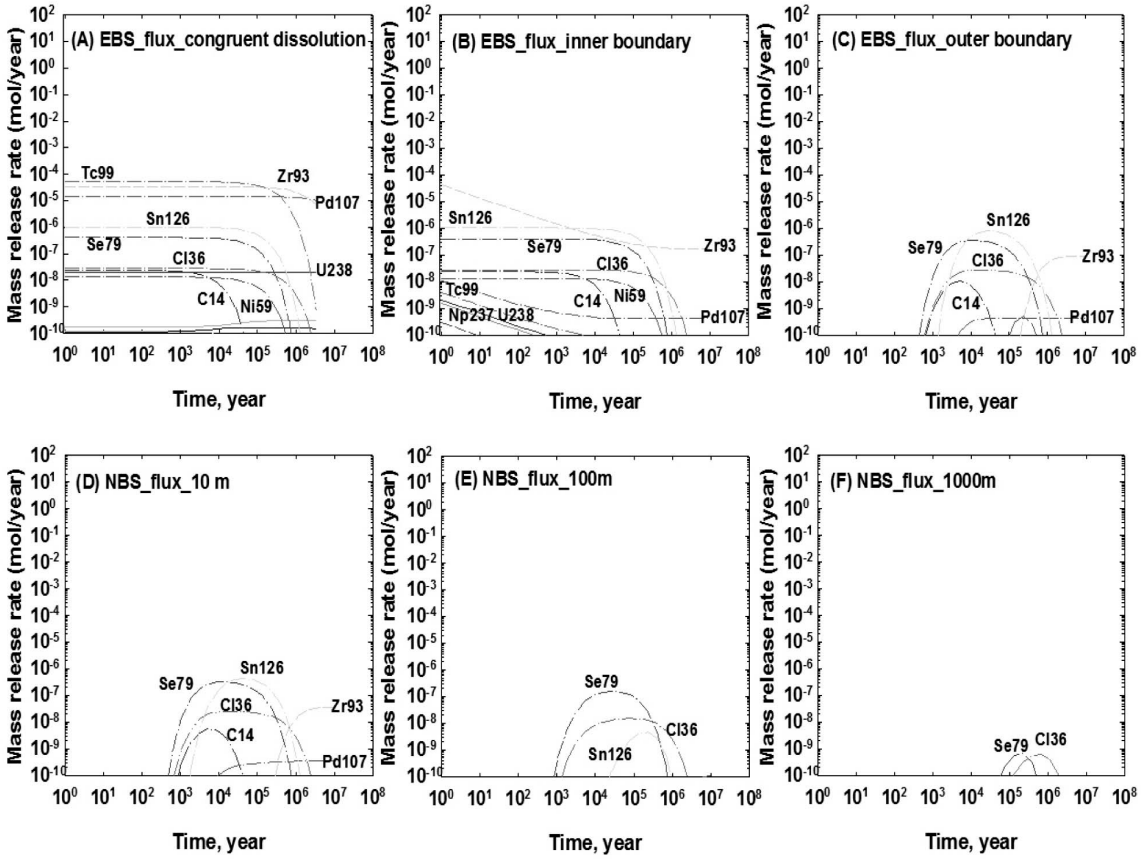

Fig. 6. The Mass Release Rate of Radionuclides at (A) the Surface of the High-level Vitrified Waste Form (Waste 3), (B) and (C) the EBS Region, and (D) through (F) in the Natural Barrier. Transport Distance through the Fractures is (D) 10 m, (E) 100 m, and (F) 1000 m. The Waste-form Alteration Time is Assumed to be 4,000,000 yr

surface as a function of time. At all three locations, the major contributor is ^{129}I, and the mass release rate of ^{135}Cs and ^{14}C are decreased with the increase of the distance. Only ^{129}I survives at the 1,000 m location.

5.1.4 Vitrified Waste (Waste Stream 5)-ILW

The intermediate-level vitrified waste form (waste 5) contains ^{90}Sr as a major nuclide (Table 1). Because the radionuclide in this waste form has a short half-life, it will decay out while it is stored at the 200 m level for at least 300 yr before final disposal.

5.1.5 Direct Disposal of Spent PWR Fuel

The spent fuel contains actinides, their daughters, and fission products as major nuclides. Most actinides and their daughters have the solubility-limited boundary conditions except ^{226}Ra, ^{241}Pu, and ^{227}Ac as shown in Table 3, and Fig. 8(A) (B). The major radionuclides observed at the inner boundary of the EBS region ($r = r_1$) are some fission products. Also most actinides and their daughters are not observed at the outer boundary of EBS, while ^{129}I, ^{135}Cs, ^{79}Se, ^{126}Sn, ^{36}Cl, and ^{93}Zr, which have long half-lives, high solubility, and no or very weak sorption distribution coefficients in the bentonite are observed as major contributors after diffusion in the EBS region. About two orders of magnitude reduction on the mass release rate of some radionuclides compare to those in the inner boundary of EBS is observed.

Figure 8 (D) through (F) show the mass release rate of radionuclides from a single waste canister at 10 m, 100 m, and 1000 m locations away from the EBS surface as a function of time. The major contributions at all locations are ^{129}I, ^{79}Se, and ^{36}Cl. Although the spent fuel as a waste form for direct disposal initially has large inventories of actinides and their daughters, none of them is a main contributor in the NBS.

5.1.6 Comparison of Different Disposal Concepts

To compare the spent PWR fuel direct disposal and the pyroprocessing waste disposal, the total mass release rates of radionuclides have been compared at the EBS surface, and in the far-field of geological formation on the same original fuel mass (26,000 MTU) basis. To get the total mass release rate of radionuclides for different

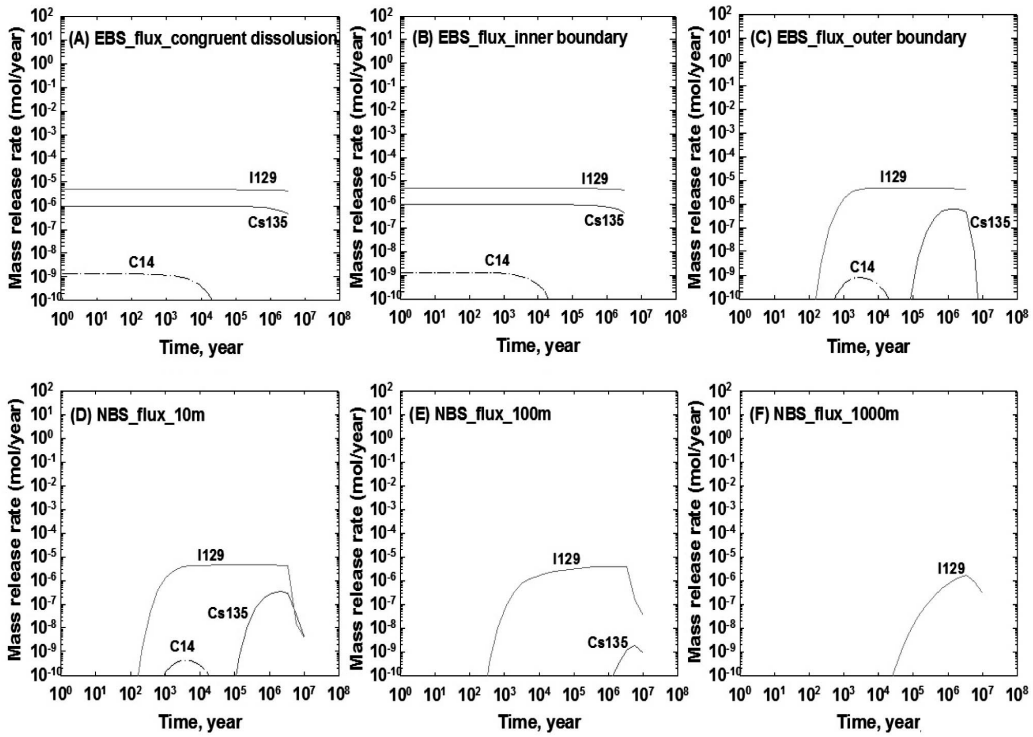

Fig. 7. The Mass Release Rate of Radionuclides at (A) the Surface of the Intermediate-level Ceramic Waste Form (Waste 4), (B) and (C) the EBS Region, and (D) through (F) in the Natural Barrier. Transport Distance through the Fractures is (D) 10 m, (E) 100 m, and (F) 1000 m. The Waste-form Alteration Time is Assumed to be 4,000,000 yr

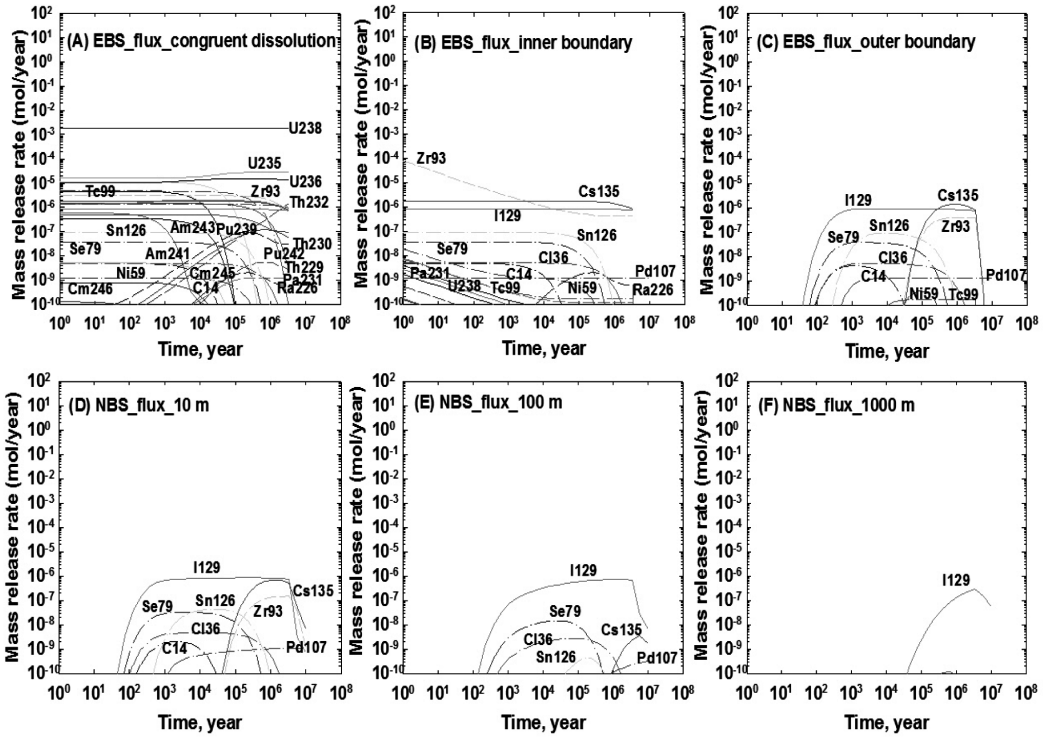

Fig. 8. The Mass Release Rate of Radionuclides at (A) the Surface of the PWR Spent Fuel, (B) and (C) the EBS Region, and (D) through (F) in the Natural Barrier. Transport Distance through the Fractures is (D) 10 m, (E) 100 m, and (F) 1000 m. The Waste-form Alteration Time is Assumed to be 4,000,000 yr

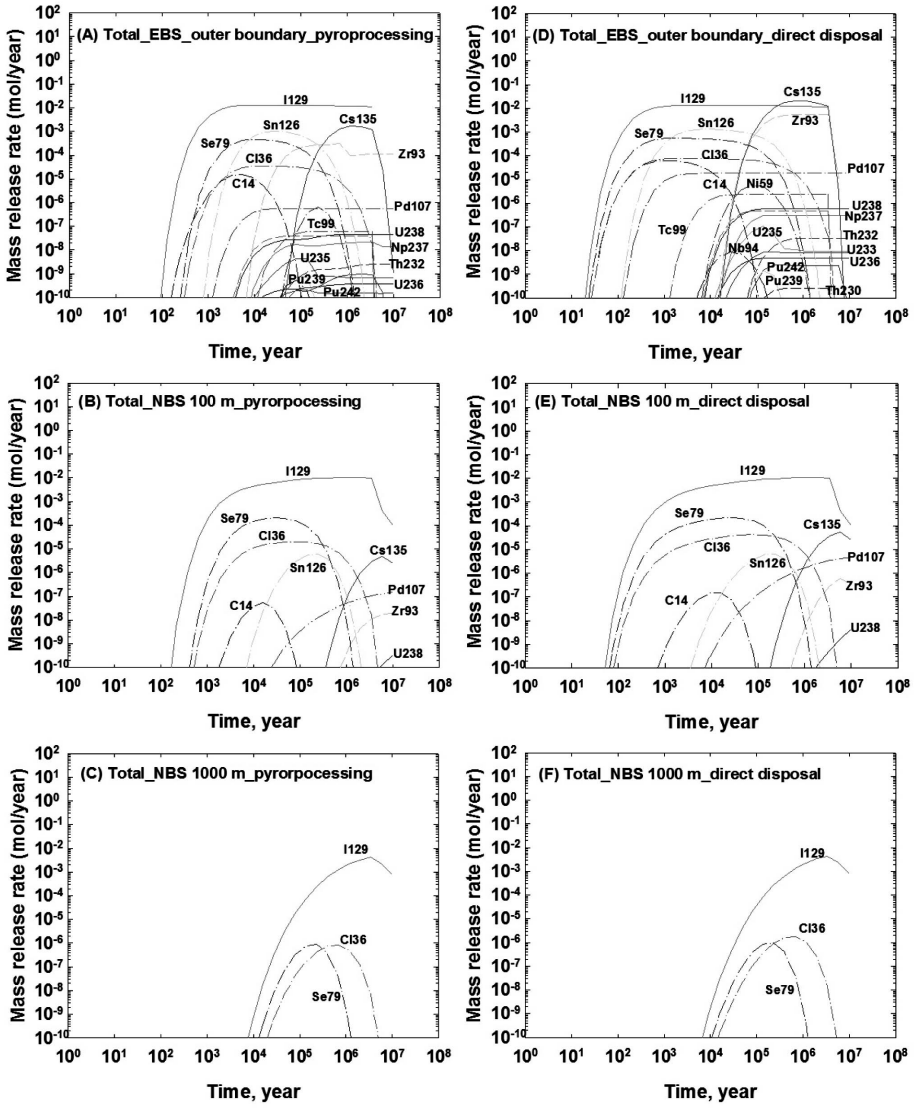

Fig. 9. The Total Mass Release Rates of Radionuclides at the Outer Boundary of EBS and at the 100 m and 1000 m Locations in NBS for the Pyroprocessing Wastes and the Spent PWR Fuels with the Waste-form Alteration time of 4,000,000 yr

waste forms from pyroprocessing, the result of the mass release rate from each single waste package was multiplied by 855, 1300, 2600, and 2600 for waste 1, waste 3, waste 4, and waste 5, respectively, and summed. In case of direct disposal, the mass release rate of a radionuclide resulting from a single waste canister has been multiplied by 14,788, which is the total number of canisters for 26,000 MTU. The results are compared in Fig. 9. The difference between these two cases compared is that uranium and TRU elements are separated for future recycle and only small fractions of these are included in waste forms from the pyroprocessing case, while all nuclides are contained in one type of canisters for the spent PWR fuel case. The assumed conditions for the waste-form alteration and radionuclide transport in the EBS and NBS are the same.

Because of the solubility-limit mechanism, only a small amount of the actinides can actually be released from the EBS to the surrounding NBS as shown in either case. Before reaching the outer boundary of the EBS, most actinide radionuclides have decayed out, while most congruently-released FP radionuclides other than short-lived ^{151}Sm and ^{137}Cs survive. Mass release rates at the EBS outer boundary for the pyroprocessing case are significantly smaller than those for the direct disposal case.

Between the EBS outer boundary and the 100-m location, such radionuclides as ^{59}Ni, ^{99}Tc, ^{237}Np, ^{239}Pu, ^{242}Pu, ^{236}U, ^{235}U, and ^{232}Th have decreased to negligible levels. Between 100m and 1,000m locations, furthermore, ^{14}C, ^{126}Sn, ^{135}Cs, ^{107}Pd, ^{93}Zr and ^{238}U become negligible. Major radionuclides

observed in the 1,000 m location are ^{129}I, ^{79}Se, and ^{36}Cl for both disposal concepts.

Note that in this evaluation we have assumed that all radionuclides released at the EBS outer boundary are injected into planar fractures in the NBS. In the NBS, radionuclides are transported through fractures associated with matrix diffusion. In the pathway, no dilution or dispersal is assumed. So, the decrease of mass release rates along the pathway occurs because of radioactive decay.

Matrix diffusion would play as a buffer during the transport through fractures [38]. It retains the contaminant plume near the entrance of the fracture. Sorption in the rock matrix strongly affects this retention mechanism. Thus, strongly-sorbing nuclides, such as ^{93}Zr, ^{135}Cs, ^{99}Tc, show significant decrease between the EBS outer boundary and the 100-m location and between the 100-m and 1,000-m locations.

5.2 Effects of Alteration Times

In this section, effects of the waste-form alteration time, T_L, for the pyroprocessing wastes are observed by a parametric study. Values of 10,000 years and 100,000 years

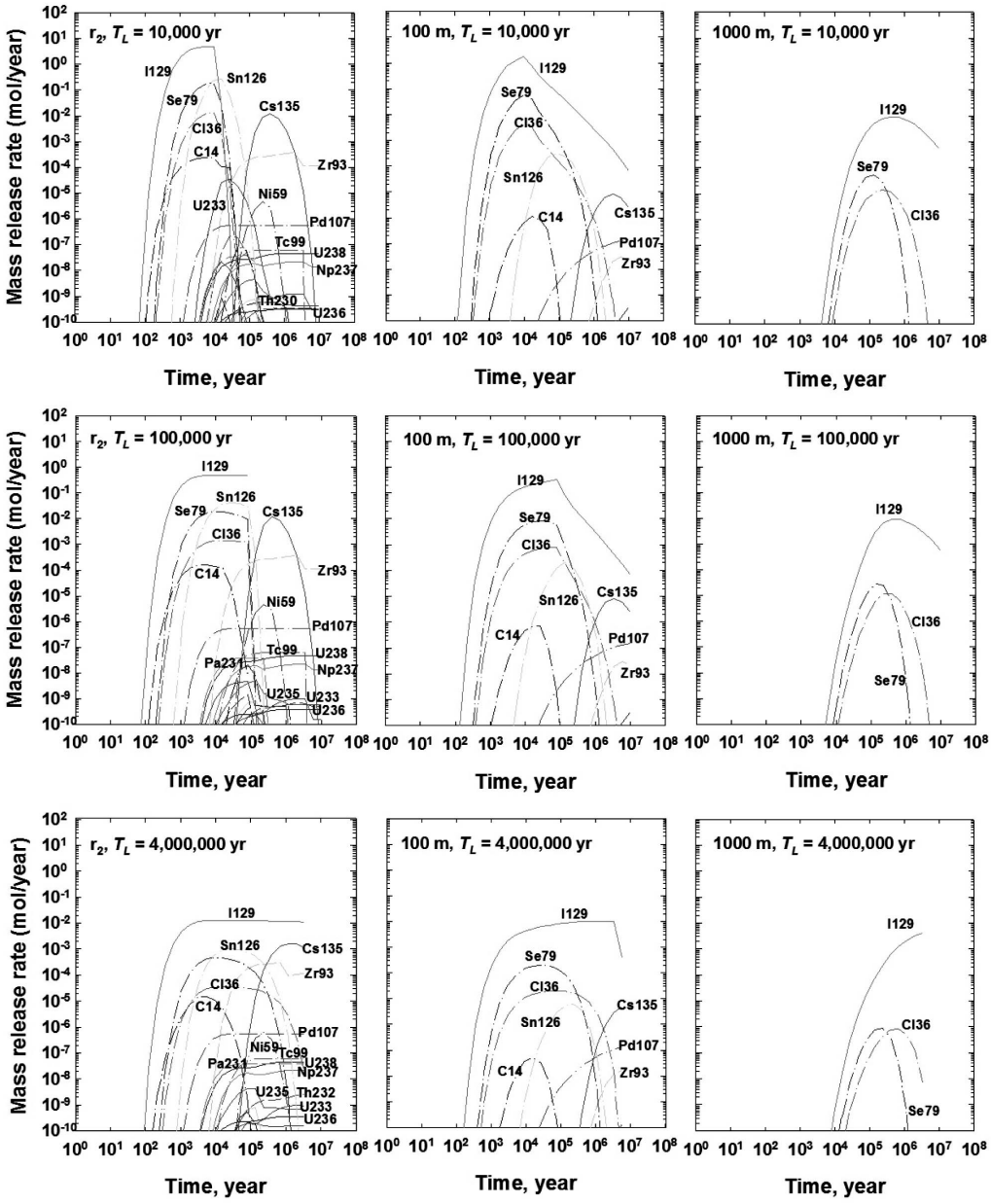

Fig. 10. The Total Mass Release Rate of Radionuclides at the Outer Boundary of EBS and at the 100 m and 1000 m Locations in NBS for T_L = 10,000 yr, 100,000 yr, and 4,000,000 yr for the Pyroprocessing Wastes

are assumed in addition to the 4 million years assumed in the previous section.

Shorter alteration times mean greater congruent release rates of radionuclides in an inversely proportional manner. This could result in generation of a precipitate at the r_1 location. For example, carbon precipitates occur for T_L = 10,000 yr case while not for T_L = 100,000 yr or for 4 million yr cases (Table 3). For solubility limited release radionuclides, among these three cases, no significant difference has been observed for the internal boundary conditions.

Figure 10 shows the total mass release rate of radionuclides released at the outer boundary of EBS region ($r = r_2$), 100 m and 1000 m of the NBS region for T_L = 10,000 yr, 100,000 yr, and 4 million yr. The effect of the waste-form alteration time, T_L, is remarkable at the outer boundary of EBS region, $r = r_2$, especially for the congruently released radionuclides. Due to faster release at the inner boundary for the shorter T_L, the peaks of these congruently release radionuclides are inversely proportionally higher, whereas the time span for the release is proportionally shorter. As the transport distance becomes longer, the difference is getting smaller because of the matrix diffusion. The release rate of the solubility-limited radionuclides is almost similar to all cases regardless of the difference in the assumed waste-form alteration time, and such radionuclides mostly decay out within the EBS.

5.3 Annual Dose Evaluation

Because the models applied here were developed primarily for the purpose of evaluating long-term safety of the repository concept, it would be interesting to compare with the regulatory guideline. Regulatory guidelines for long-term safety of Korean repository concepts for SNF and HLW are yet to be established, while the Korean regulatory guideline for the long-term safety for the low-level waste disposal is set at 0.1 mSv/year for general scenario [39]. To calculate the annual dose, we have adopted the dose coefficients (Sv/Bq) for ingestion from ICRP Publication 72 [40]. In the present calculation, the fractional absorption in the gastrointestinal tract is conservatively set to be unity.

For more complete evaluation, we need to continue the transport analysis in the geosphere until radionuclides enter the biosphere, and then to perform the pathway analysis in the biosphere based on assumed food-chain conditions and irradiation scenarios, such as ingestion, inhalation, and external radiation. However, at this point of time, both repository concepts are generic; we do not know where the repository would be sited. We do not have sufficient information to perform a more complete dose evaluation. The purpose of the present stylized evaluation is to understand what level of confinement could be achieved by the present systems we consider.

Here, we utilize the numerical results for the mass release rates (mol/year) at the 1,000-m location in the NBS, shown in Figs. 9 and 10. The annual dose has been calculated by first converting the mass release rate into the radioactivity release rate (Bq/year), and then by multiplying the dose coefficients (Table 4) by the radioactivity release rate. Note that the annual dose has been obtained under the following assumptions: (1) no radionuclides are lost due to dispersal or dilution during the transport, and (2) all radionuclides reaching this location would be ingested. In more comprehensive evaluations, the annual dose is evaluated by multiplying the dose coefficient by the annual amount of radioactivity taken by a human being. Thus, the results shown below can be considered as an extremely conservative worst case.

Table 4. Ingestion dose coefficients (Sv/Bq)

Radionuclide	Ingestion dose coefficients (Sv/Bq)
^{36}Cl	9.3E-10
^{79}Se	2.9E-09
^{129}I	1.1E-07

* data from Ref. [40]

Figure 11 shows the annual dose for different values of T_L = 10,000 yr, 100,000 yr, and 4 million yr for pyroprocessing case and T_L = 4 million yr for direct disposal of spent PWR fuel case. These figures indicate that for these radionuclides, particularly ^{129}I and ^{79}Se, we need to account for some mechanisms of dilution or dispersal during the transport through the geosphere and the biosphere. The results for ^{36}Cl indicate that by solidifying this nuclide in a robust waste form that lasts more than a million years, radiological impact of this nuclide is negligible even under such extreme conservatism.

6. DISCUSSION

In the current model approach, there are some limitations and simplifications that would considerably affect observations we have shown above.

First, we simplified the EBS region as a homogeneous porous region. The effects of metal canister containing waste form and the packages containing canisters are considered only by the package failure time of 1,000 yr in this analysis. We assumed the common waste-form alteration time for all waste forms and neglected all coupled effects among materials included in the EBS. The detailed structure of the EBS would affect the time when radionuclide release starts and how radionuclides are transported in the EBS. The current model is still considered to be conservative in that it gives the shortest transport time of radionuclides. The present analysis shows that the A-KRS for the pyroprocessing wastes could achieve at least the same level of the long-term safety as the KRS system for spent PWR fuel. But, if the main question of interest

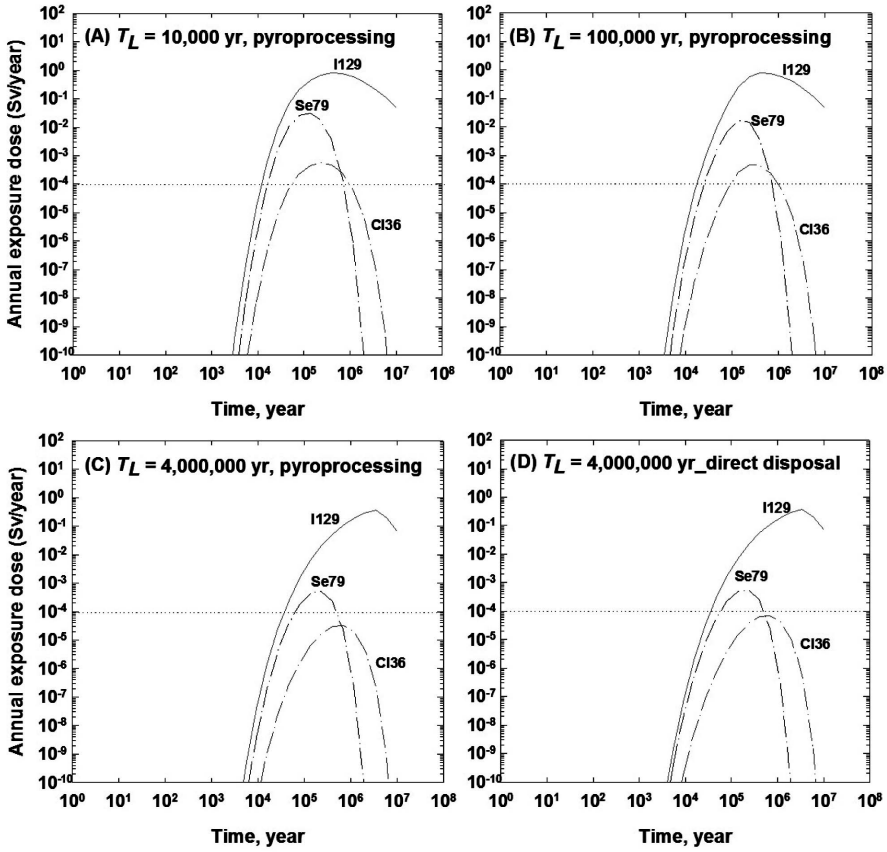

Fig. 11. Comparison of Annual Doses Between the KIEP-21 System and Direct Disposal of Spent PWR Fuel Case. Dashed Lines Indicate the Korean Regulatory Guideline for the Long-term Safety for the Low-level Waste Disposal

is which system is better or how much better between the two systems, then we need to incorporate detailed design specification of the EBS in our analysis, and investigate if and how such details would affect the repository performance. Another important note is that uncertainties must be taken into account for such comparison. This is the task we are currently working for.

As shown in the numerical results in this study, regardless of whether the waste form contains a certain amount of actinides or not, main contributors at the NBS are not actinides but some fission products such as ^{129}I, ^{79}Se, and ^{36}Cl. This is because actinides have extremely low solubilities in the reducing environment, and only a small amount of the actinides can actually be released from the EBS to the surrounding geologic formations. ^{129}I survives the transport in the far-field region without significant reduction because of its long half-life and weak sorption. The congruent release assumption for waste 4 is reasonable because of homogeneous solidification of iodine in this waste form. For this case, the magnitude of the peak radiological impact by ^{129}I is determined by the durability of the ceramic waste form. For the spent PWR case, the release of ^{129}I would be earlier and faster than the congruent release assumed in this analysis because of higher burn-up effect in the peripheral region in the fuel pellets, so-called rim effects.

While the total mass release rate of radionuclides from direct disposal concept is almost similar to those from the pyroprocessing disposal concept, we should pay attention to the difference in the total repository footprint. In case of A-KRS with the pyroprocessing, 28 tunnels (i.e., 1 tunnel for metal waste form, 16 tunnels for high-level vitrified waste form, 9 tunnels for intermediate-level ceramic waste form, and 2 tunnels for intermediate-level vitrified waste form; tunnels for the high-level ceramic waste form (waste 2) are left out of account) with 150 (L) $\times 8$ (W) $\times 8$ (H) dimension are needed to dispose of the wastes from 26,000 MTU. Also the A-KRS disposal system for pyroprocessing should be constructed at two separate levels: one shallow level at 200 meter is for the waste with no decay heat and the other deep level at 500 meter is for the HLW [13]. On the other hand, 420 tunnels with 251 (L) $\times 5$ (W) $\times 6.15$ (H) dimension are needed for the direct disposal concept to dispose the same amount of spent fuel. The disposal footprint of repository for the whole wastes from the pyroprocessing is about one tenth

of those for the whole wastes from the direct disposal. This is expected to result in considerable cost saving for repository construction. A natural question would be if this cost saving can pay off the cost of the pyroprocessing. To answer this question, we need to develop an economics model including the pyroprocessing system and the A-KRS and supporting facilities as well as institutional and operational costs for various facilities.

For more complete and fair comparison between these two concepts, the recycle of separated uranium and TRU in the KIEP-21 should have been included in the present analysis. With an advanced fast-spectrum reactor, these materials could have generated additional electricity, while generating additional ILW and HLW. This means that with the same 26,000 MTU much greater electricity could be obtained. The comparison between two concepts should be made on the same electricity basis. This is, however, beyond the scope of the present study, and will be addressed in future studies.

7. CONCLUSIONS

In the present study, we have performed a scoping parametric study to survey effects of different waste forms in different repository designs by comparing the case of direct disposal of spent PWR fuel in the KRS concept with the case of A-KRS repository containing ILW and HLW from the KIEP-21 system. By determining the boundary conditions for the multiple-member decay chains of actinides and fission products based on the analysis of precipitation at the waste-form alteration location, numerical evaluations have been made for actinide and fission products transport in the EBS and in the surrounding NBS. Utilizing the mass release rate at the 1,000-m location, the annual dose has been evaluated for various waste-form alteration times, and compared with the existing Korean safety guideline.

Both in the pyroprocessing disposal concept and the direct disposal concept, most actinides and their daughters remain as precipitates in the EBS because of their assumed low solubilities. Therefore, the radionuclides that reach to the 1000-m location are such fission products as ^{129}I, ^{79}Se, and ^{36}Cl. They have high solubilities and weak sorption with the EBS materials or with the host rock, and are released congruently with waste-form alteration. For the assumed conditions and parameter values, it has been observed that the total mass release rates of radionuclides from the direct disposal concept are similar to those from the pyroprocessing disposal concept.

The effects of the waste-form alteration rate on the release of radionuclides from the EBS boundary have been found to be significant, especially for congruently released radionuclides. Because the waste-form alteration rate and subsequent radionuclide release rate from the EBS are influenced and determined by the design and evolving environment of the EBS, it is imperative to understand the evolution of materials in this region. Particularly, it is recommended to develop a better waste form and to improve understanding of dissolution and release of ^{129}I, ^{79}Se, and ^{36}Cl from the corresponding waste forms.

Nevertheless, because the baseline long-term radiological repository safety has been confirmed by the dose evaluation to be achieved by either combination (KRS + spent PWR fuel or A-KRS + Pyro wastes), the repository optimization should be sought for other aspects, such as costs, retrievability, reversibility, and overall flexibility of the materials management in the fuel cycle. For example, for repository footprint, the advantage of the pyroprocessing disposal concept over the direct disposal concept is obvious. It would be even more if we take into account additional electricity to be generated by the recycle of separated U and TRU in the KIEP-21.

To make more decisive conclusions, however, we need further studies with models with high fidelity and reality for the coupled phenomena among waste forms, EBS materials, groundwater, and radionuclides. We also need to make an economic analysis to make judgments for the overall advantage of the pyroprocessing and A-KRS systems.

ACKNOWLEDGMENTS

The authors are grateful for Dr. Eung Ho Kim of Korea Atomic Energy Research Institute for his stimulating discussions and reviewing our draft. We also appreciate advice and help by Dr. Youn-Myoung Lee and Dr. Yongsoo Hwang also of KAERI.

REFERENCES

[1] MKE, "National Energy Basic Plan, 2008," *Korean Ministry of Knowledge Economy*, Press Release (August 28, 2008).

[2] W. I. Ko and E. Kwon, "Implications of the new National Energy Basic Plan for nuclear waste management in Korea," *Energy Policy*, **37**, 3484 (2009).

[3] L. H. Johnson and D. W. Shoesmith, *Spent fuel. In: W. Lutze and R.C. Ewing* (*eds.*) *Radioactive waste form for the future*, p. 635-698, Elsevier Science Publishers, B.V., Amsterdam (1988).

[4] S. V. Stefanovsky, S. V. Yudintsev, R. Giere, and G. R. Lumpkin, *Nuclear waste forms. In: R. Giere and P. Stille (eds.) Energy, Waste, and the Environment: a Geochemical Perspective*, Geological Society, Special Publications, **236**, p 37-63, London (2004).

[5] K. J. Lee, "Spent fuel management with pyroprocessing _The advantages of the pyroprocessing optioin from the perspective of waste management," *KAERI Nuclearancy*, **1**, 8 (2008).

[6] KAERI, "Advanced Nuclear Fuel Cycle," *KAERI Newsletter* (Winter 2008).

[7] Y. Hwang, ed., "Summary of the KAERI's KIEP-21 Pyro-processing, v0.5," Korean Atomic Energy Research Institute, Republic of Korea (March 2009).

[8] J. Ahn, "Integrated radionuclide transport model for a high-level waste repository in water-saturated geological formations," *Nucl. Technol*., **121**, 24 (1998).

[9] J. Choi, S. Kwon, C. Kang, and Y. Kwon, "A Reference Container Concept for Spent Fuel Disposal: Structural safety for dimensioning of the reference container," *J. Korean Assoc. Rad. Prot*, **29**, 49 (2004).
[10] J. Lee, D. Cho, H. Choi, and J. Choi, "Concept of a Korean reference disposal system for spent fuels," *J. Nucl. Sci. Technol*., **44**, 1565 (2007).
[11] J. Kim, Y. Koh, D. Bae, and J. Choi, "Depth and layout optimizations of a radioactive waste repository in a discontinuous rock mass based on a thermomechanical model," *Nucl. Eng. Technol*., **40**, 429 (2008).
[12] J. O. Lee, J. H. Park, and W. J. Cho, "Engineering-scale test on the thermal-hydro-mechanical behaviors in the clay barrier of a HLW repository," *Ann. Nucl.Eenergy*, **35**, 1386 (2008).
[13] KAERI, "Development of three disposal options for HLW from pyroprocessing of PWR spent fuels, v2.1," Korean Atomic Energy Research Institute (2008).
[14] Y. Hwang, "Review on KIEP-21," Korean Atomic Energy Research Institute, Republic of Korea (March 2009).
[15] H. S. Park, I. T. Kim, Y. Z. Cho, H. C. Eun, and J. H. Kim, "Characteristics of Solidified Products Containing Radioactive Molten Salt Waste," *Environ. Sci. Technol*., **41**, 7536 (2007).
[16] H. S. Park, I. T. Kim, H. Y. Kim, S. K. Ryu, and J. H. Kim, "Stabilization/Solidification of Radioactive Molten Salt Waste via Gel-Route Pretreatment," *Environ. Sci. Technol*., **41**, 1345 (2007).
[17] H. S. Park, I. T. Kim, Y. Z. Cho, H. C. Eun, and H. S. Lee, "Stabilization/Solidification of Radioactive Salt Waste by Using $xSiO_2$-yAl_2O_3-zP_2O_5 (SAP) Material at Molten Salt State," *Environ. Sci. Technol*, **42**, 9357 (2008).
[18] E. H. Kim, G. I. Park, Y. Z, Cho, and H. C. Yang, "A new approach to minimize pyroprocessing waste salts through a series of fission product removal process," *Nucl. Technol*., **162**, 208 (2008).
[19] J. H. Yoo, C. S. Seo, E. H. Kim, and H. S. Lee, "A conceptual study of pyroprocessing for recovering actinides from spent oxide fuels," *Nucl. Eng. Technol*., **40**, 581 (2008).
[20] E. H. Kim, "Flowsheet study for a pyroprocess of an oxide to a metal (Korea)," Korean Atomic Energy Research Institute, Republic of Korea (2007).
[21] Y. J. Cho, H. C. Yang, H. C. Eun, E. H. Kim, and I. T. Kim, "Characteristics of oxidation reaction of rare-earth chlorides for precipitation in LiCl-KCl molten salt by oxygen sparging," *J. Nucl. Sci. Technol*., **43**, 1280 (2006).
[22] Y. Z. Cho, H. C. Yang, G. H. Park, H. S. Lee, and I. T. Kim, "Treatment of a waste salt delivered from an electrorefining process by an oxidative precipitation of the rare earth elements," *J. Nucl. Mat*., **384**, 256 (2009).
[23] C. H. Kang, J. U. Gu, S. G. Kim, S. S. Kim, J. H. Kim, J. H. Park, Y. M. Lee, J. W. Lee, G. S. Jeon, W. J. Cho, J. W. Choi, Y. Hwang, and S. G. Kwon, "High-level radwaste disposal technology development - Geological disposal system development," KAERI/RR/2013/99, Korean Atomic Energy Research Institute (1999).
[24] C. H. Kang, J. W. Kim, G. S. Jeon, J. H. Park, W. J. Cho, J. W. Choi, J. W. Lee, Y. M. Lee, S. S. Kim, Y. Hwang, S. G. Kim, and S. G. Kwon, "High-Level Radwaste Disposal Technology Development - Geological disposal system development," KAERI/RR-2336/2002, Korean Atomic Energy Research Institute (2002).
[25] KBS, "Final storage of spent nuclear fuel- KBS-3. Summary," SKBF/KBS (1983).
[26] M. H. Baik, S. Y. Lee, J. K. Lee, S. S. Kim, C. K. Park, and J. W. Choi, "Review and compilation of data on radionuclide migration for the performance assessment of a HLW repository in Korea," *Nucl. Eng. Technol*., **40**, 593 (2008).
[27] W. J. Cho, J. O. Lee, K. S. Chun, and D. S. Hahn, "Basic Physicochemical and Mechanical Properties of Domestic Bentonite for Use as a Buffer Material in a High-level Radioactive Waste Repository," *J. Korean Nucl. Soc*., **31**, 39 (1999).
[28] Y. Hwang, "Copper canister lifetime limited by a sulfide intrusion in a deep geologic repository," *Prog. Nucl. Energy*, **51**, 695 (2009).
[29] J. Ahn, T. Ikeda, T. Ohe, T. Kanno, Y. Sakamoto, T. Chiba, M. Tsukamoto, S. Nakayama, S. Nagasaki, K. Banno, and T. Fujita, "Quantitative performance allocation of multi-barrier system for high-level radioactive waste disposal," *J. Atomic Energy Soc. Japan*, **37**, 59 (1995).
[30] Y. M. Lee, C. H. Kang, and Y. Hwang, "Nuclide release from an HLW repository: Development of a compartment model," *Ann. Nucl. Energy*, **34**, 782 (2007).
[31] KAERI, KAERI_PyroInformation19May2009.xls. (2009).
[32] KAERI, KAERI_Input_Data.xls. (2007).
[33] J. Bruno and R. C. Ewing, "Spent Nuclear Fuel," *ELEMENTS*, **2**, 343 (2006).
[34] E.C. Buck, B.D. Hanson, and B.K. McNamara, The geochemical behavior of Tc, Np, and Pu in spent nuclear fuel in an oxidizing environment. In: R. Giere, P. Stille (eds) *Energy, Waste, and the Environment: a Geochemical Perspective*, The Geological Society of London Special Publication (2004).
[35] D. J. Ashworth, G. Shaw, A. P. Butler, and L. Ciciani, "Soil transport and plant uptake of radio-iodine from near-surface groundwater," *J. Environ. Radioact*., **70**, 99 (2003).
[36] X. L. Hou, C. L. Fogh, J. Kucera, K. G. Andersson, H. Dahlgaard, and S. P. Nielsen, "Iodine-129 and Caesium-137 in Chernobyl contaminated soil and their chemical fractionation," *Sci Total Environ*, **308**, 97 (2003).
[37] D. I. Kaplan, G. Iverson, S. Mattigid, and K. Parker, "^{129}I - Test and Research to Support Disposal Decisions," WSRC-TR-2000-00283, Pacific Northwest National Laboratory (2000).
[38] J. Ahn, "Mass Transfer and Transport of Radionuclides in Fractured Porous Rock," PhD Dissertation, University of California, Berkeley (1988).
[39] MEST, "Korean Third National Report under the Joint Convention on the Safety of Spent Fuel Management and on the Safety of Radioactive Waste Management", *Korean Ministry of Education, Science, and Technology* (October, 2008)
[40] ICRP (International Commission on Radiological Protection), ICRP publication 72_*Age-dependent Doses to Members of the Public from Intake of Radionuclides: Part 5. Compilation of Ingestion and Inhalation Dose Coefficients*, Pergamon Press, Oxford (1996).
[41] M. Benedict, T. H. Pigford, and H. W. Levi, *Nuclear chemical engineering*, **2nd ed**., Appendix C. McGraw-Hill Book Company, New York (1981).